Geophysical Research Letters

RESEARCH LETTER
10.1029/2018GL081685

Deep Argo Quantifies Bottom Water Warming Rates in the Southwest Pacific Basin

Gregory C. Johnson[1], Sarah G. Purkey[2], Nathalie V. Zilberman[2], and Dean Roemmich[2]

[1]Pacific Marine Environmental Laboratory, NOAA, Seattle, WA, USA, [2]Scripps Institution of Oceanography, University of California, San Diego, La Jolla, CA, USA

Key Points:
- Deep and bottom waters in the Southwest Pacific Basin from 2014 to 2018 are increasingly warmer than climatology with increasing depth
- The warm anomaly is statistically different from zero at pressures >2,800 dbar and reaches 11 (±1) m°C by 5,500 dbar (1 m°C = 0.001 °C)
- Deep Argo floats measure a regional mean warming rate of about 3 (±1) m°C/year from 5,000 to 5,600 dbar and from 2014 to 2018

Correspondence to:
G. C. Johnson,
gregory.c.johnson@noaa.gov

Citation:
Johnson, G. C., Purkey, S. G., Zilberman, N. V., & Roemmich, D. (2019). Deep Argo quantifies bottom water warming rates in the Southwest Pacific Basin. *Geophysical Research Letters*, *46*, 2662–2669. https://doi.org/10.1029/2018GL081685

Received 13 DEC 2018
Accepted 11 FEB 2019
Accepted article online 13 FEB 2019
Published online 7 MAR 2019

Abstract Data reported from mid-2014 to late 2018 by a regional pilot array of Deep Argo floats in the Southwest Pacific Basin are used to estimate regional temperature anomalies from a long-term climatology as well as regional trends over the 4.4 years of float data as a function of pressure. The data show warm anomalies that increase with increasing pressure from effectively 0 near 2,000 dbar to over 10 (±1) m°C by 4,800 dbar, uncertainties estimated at 5–95%. The 4.4-year trend estimate shows warming at an average rate of 3 (±1) m°C/year from 5,000 to 5,600 dbar, in the near-homogeneous layer of cold, dense bottom water of Antarctic origin. These results suggest acceleration of previously reported long-term warming trends in the abyssal waters in this region. They also demonstrate the ability of Deep Argo to quantify changes in the deep ocean in near real-time over short periods with high accuracy.

Plain Language Summary The coldest waters that fill much of the deep ocean worldwide originate near Antarctica. Temperature data collected from oceanographic cruises around the world at roughly 10-year intervals show that these near-bottom waters have been warming on average since the 1990s, absorbing a substantial amount of heat. Data from an array of robotic profiling Deep Argo floats deployed in the Southwest Pacific Ocean starting in mid-2014 reveal that near-bottom waters there have continued to warm over the past 4.4 years. Furthermore, these new data suggest an acceleration of that warming rate. These data show that Deep Argo floats are capable of accurately measuring regional changes in the deep ocean. The ocean is the largest sink of heat on our warming planet. A global array of Deep Argo floats would provide data on how much Earth's climate system is warming and possibly improve predictions of future warming.

1. Introduction

One of the more striking results of analyses of data from decadal repeat hydrographic sections by GO-SHIP (Talley et al., 2016) may be the large-scale warming of the abyssal (depth > 4,000 m) waters (Desbruyères et al., 2016; Kouketsu et al., 2011; Purkey & Johnson, 2010) and Southern Ocean freshening of some Antarctic Bottom Waters (e.g., Aoki et al., 2013; Purkey & Johnson, 2013; Rintoul, 2007) since the World Ocean Circulation Experiment survey in the 1990s. These abyssal waters are ventilated primarily by Antarctic Bottom Waters that are formed when very cold, dense waters on the Antarctic continental shelf descend along the continental slope, entraining warmer, lighter, older Circumpolar Deep Waters as they flow into the abyssal ocean (Orsi et al., 1999). Antarctic Bottom Waters, albeit diluted to the north, fill the majority of the abyssal ocean and account for a substantial fraction of the deep (2,000–4,000 m) ocean waters as well (Johnson, 2008). The observed warming and freshening signals are largest around Antarctica, where these bottom waters are formed, but the warming is also found throughout much of the global ocean. This Antarctic Bottom Water warming signal also arises in high-resolution climate models under increased greenhouse gas forcing (Newsom et al., 2016), suggesting the possibility of future increases in abyssal ocean heat storage.

Ocean warming accounted for about 93% of the excess heat building up in the climate system from 1971 to 2010 as a result of anthropogenic climate forcing (Rhein et al., 2013), mostly CO_2 emissions from burning fossil fuels (Hartmann et al., 2013). Since the Intergovernmental Panel on Climate Change's Fifth Assessment Report, near-global (first sparsely in 2005), year-round, high-quality temperature-salinity profiles from the surface to about 2,000 dbar collected by Argo floats have afforded an increasingly accurate estimate of decadal global mean ocean warming rates in that upper half of the ocean volume, with 5–95% uncertainty now about ±1/6th of the decadal rate estimate (e.g., Johnson et al., 2016;

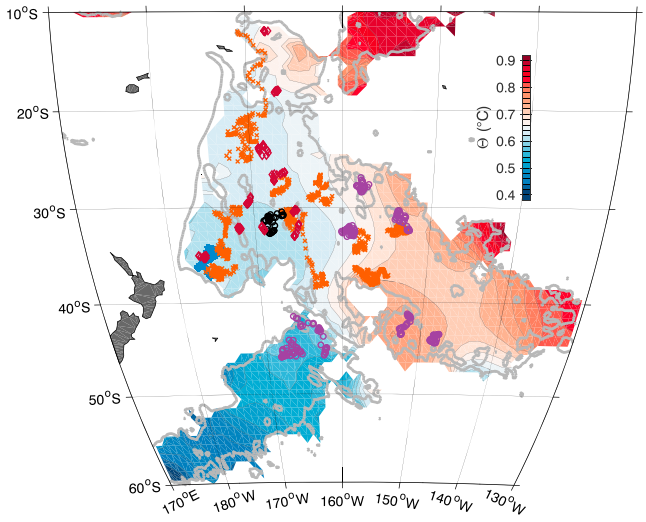

Figure 1. Locations of Deep Argo float profiles in the Southwest Pacific Basin as of 20 November 2018 deployed in 2014 (blue plus symbols), 2016 (orange cross symbols), 2017 (purple circles, except black circles around 32°S, 168°W for float WMO 5902528), and 2018 (red diamonds) with climatological conservative temperature Θ values from World Ocean Atlas 2018 (https://www.nodc.noaa.gov/OC5/woa18/) contoured at 0.02 °C intervals (see color bar) at 5,000 m. The 5,000-m isobath (thick gray line) is contoured from ETOPO1 (Smith & Sandwell, 1997) smoothed with a 30′ × 30′ half-width hanning filter.

Roemmich et al., 2015). The lower half of the ocean, which is globally sparsely surveyed at decadal intervals, also appears to take up a substantial amount of heat, accounting for about 6% of the total global ocean heat uptake rate since 1993, but the 5–95% uncertainties for the deep warming are roughly the same size as the signal (Johnson et al., 2018).

The relation between ocean warming and future atmospheric warming in climate models (e.g., Boé et al., 2009), as well as the importance of patterns of deep ocean warming and freshening to regional sea level budgets and sea level rise (e.g., Purkey et al., 2014), motivates a global Deep Argo array. Deep Argo floats are a revolutionary new technology that allows autonomous ocean robots to measure vertical profiles of temperature and salinity from the ocean surface to pressures as high as either 4,000 or 6,000 dbar (depending on the model) and sample to within a few meters of the ocean floor, closer than that achieved from ships. One design study (Johnson et al., 2015) suggests that a global array of 1,224 Deep Argo floats (nominal 5° latitude × 5° longitude spacing in the seasonally ice-free ocean deeper than 2,000 dbar) profiling from the ocean surface to the seafloor would reduce uncertainties of global estimates of deep warming by a factor of 5 compared to warming estimates made only with GO-SHIP decadal repeat oceanographic sections. Deep Argo regional pilot arrays are already underway to demonstrate feasibility of deploying the floats, build the capacity to do so, and illustrate usefulness of the data (Jayne et al., 2017; Kobayashi, 2018).

Here we analyze data from one of those Deep Argo regional pilot arrays, specifically 31 Deep Argo floats deployed in the Southwest Pacific Basin (Figure 1), two as early as June 2014, to quantify regional deep ocean temperature changes in the region. In section 2 we introduce the climatology and Argo data used, as well as our methods for analyzing the basin-averaged temperature differences from climatology, array length trends, and their confidence limits. In section 3 we present the results, and in section 4 we discuss them. We demonstrate that even this modest array of floats can detect statistically significant differences from a long-term climatology, as well as trends over 4.4 years or less, in the deep and abyssal Southwest Pacific Basin.

2. Data and Methods

We use the World Ocean Atlas 2018 (WOA18) for a temperature and salinity climatology (https://www.nodc.noaa.gov/OC5/woa18/). From WOA18 long-term values of temperature, practical salinity, and depth, we calculate absolute salinity (S_A) and conservative temperature (Θ) using TEOS-10 (IOC, SCOR and IAPSO, 2010) for the equation of state.

We downloaded Deep Argo data in the Southwest Pacific Basin from an Argo Global Data Assembly Center (http://doi.org/10.17882/42182) on 20 November 2018. There were 31 floats that had sampled in the region as of that date. Two were deployed in 2014, 11 in 2016, 8 in 2017, and 10 more in 2018. These floats provided a total of 1,914 profiles (Figures 1 and 2), with 1,514 of those reaching a pressure of 3,900 dbar, 1,375 reaching a pressure of 4,800 dbar, and 388 reaching a pressure of 5,500 dbar (Figure 3a). We used the Argo adjusted values of temperature, practical salinity, and pressure (or the unadjusted values where the adjusted were unavailable), linearly interpolating the data (which were sampled by the floats at a variety of vertical resolutions from continuously to 5-, 10-, 20-, or 50-dbar intervals) to a uniform grid at 100-dbar intervals, the latter being similar to the WOA18 100-m vertical spacing from 2,000 to 5,500 m.

The temperature sensors for the SeaBird Scientific SBE-61 CTDs (Conductivity-Temperature-Depth instruments) used on these Deep Argo floats were carefully selected to exhibit less than 1 m°C/year (1 m°C = 0.001 °C) drift prior to delivery. Even thermistors used for SBE-41 CTDs on core Argo floats that have been recovered after years in the field have held their calibration to order 1 m °C (e.g., Oka & Ando, 2004). Here we focus on analysis of the Θ profiles, since the temperature data are thought to be very accurate and stable, whereas the salinity data have not yet been subject to delayed mode scientific quality control,

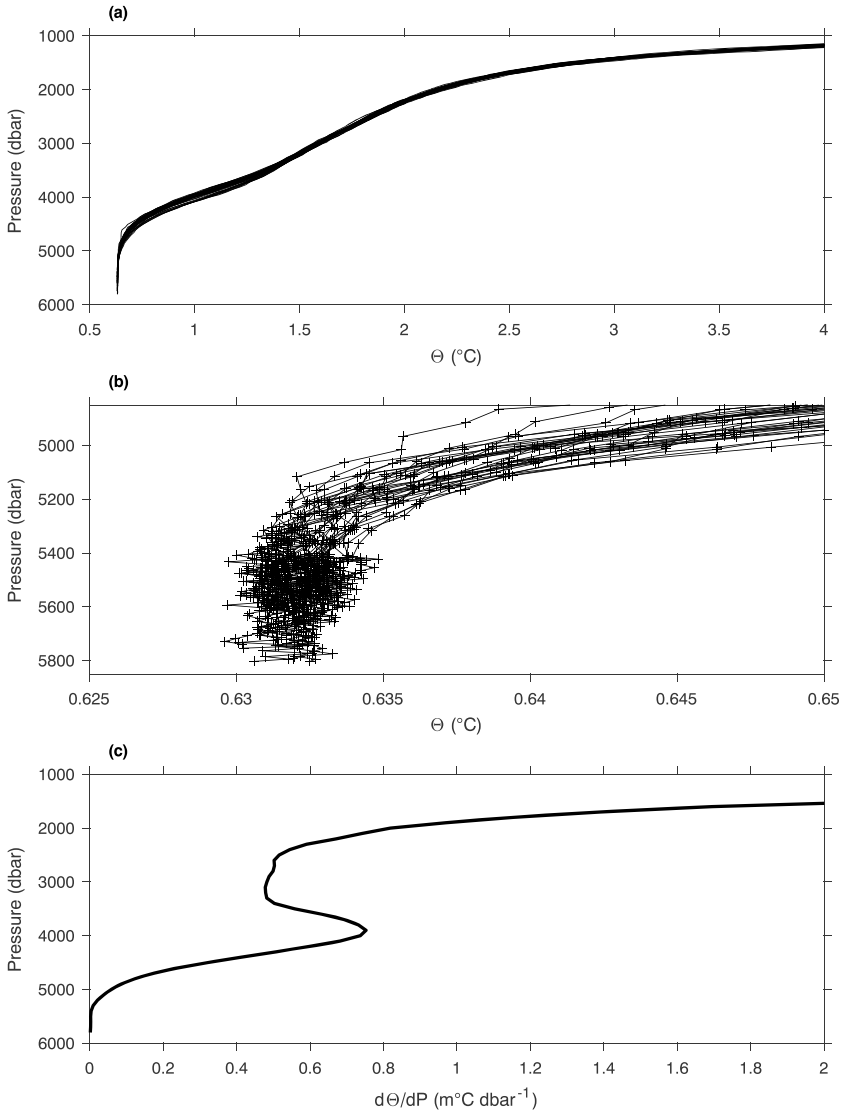

Figure 2. Profiles versus pressure (P, dbar) of (a) conservative temperature (Θ; °C) for Deep Argo float WMO 5902528 (see black circles in Figure 1 for profile locations) from 1,000 dbar to the bottom (thin black lines), (b) from 4,850 dbar to the bottom with individual data points indicated (black plus symbols), and (c) ensemble mean (thick black line) of conservative temperature vertical gradients (dΘ/dP; m°C) calculated from each profile.

and a very high level of accuracy and stability is needed to study salinity changes in the deep ocean (e.g., Purkey & Johnson, 2013).

We fit a sixth-order polynomial to float practical salinity data as a function of temperature for all the interpolated float data at pressures of 900 dbar and greater. If the float practical salinity values deviated by more than 0.1 PSS-78 from that fit, the salinity from the fit was used rather than that reported by the float. This step eliminated a small number of bad salinity values arising either from rapid measurement drift in one of the CTDs or an impedance mismatch between the CTD and the float controllers in a few of the early models. It introduces no more than a 1-m°C error in affected Θ values. We then calculated S_A, Θ, and depth from the salinity, temperature, and pressure data. Pressure calibration errors and pressure sensor drift may also be a concern, but the impacts of those are small in the nearly vertically homogeneous bottom layer.

For each Argo data point we calculate anomalies of Θ from WOA18 by linear interpolation in latitude-longitude depth coordinates. Where linear interpolation is not possible, the data points are discarded. For

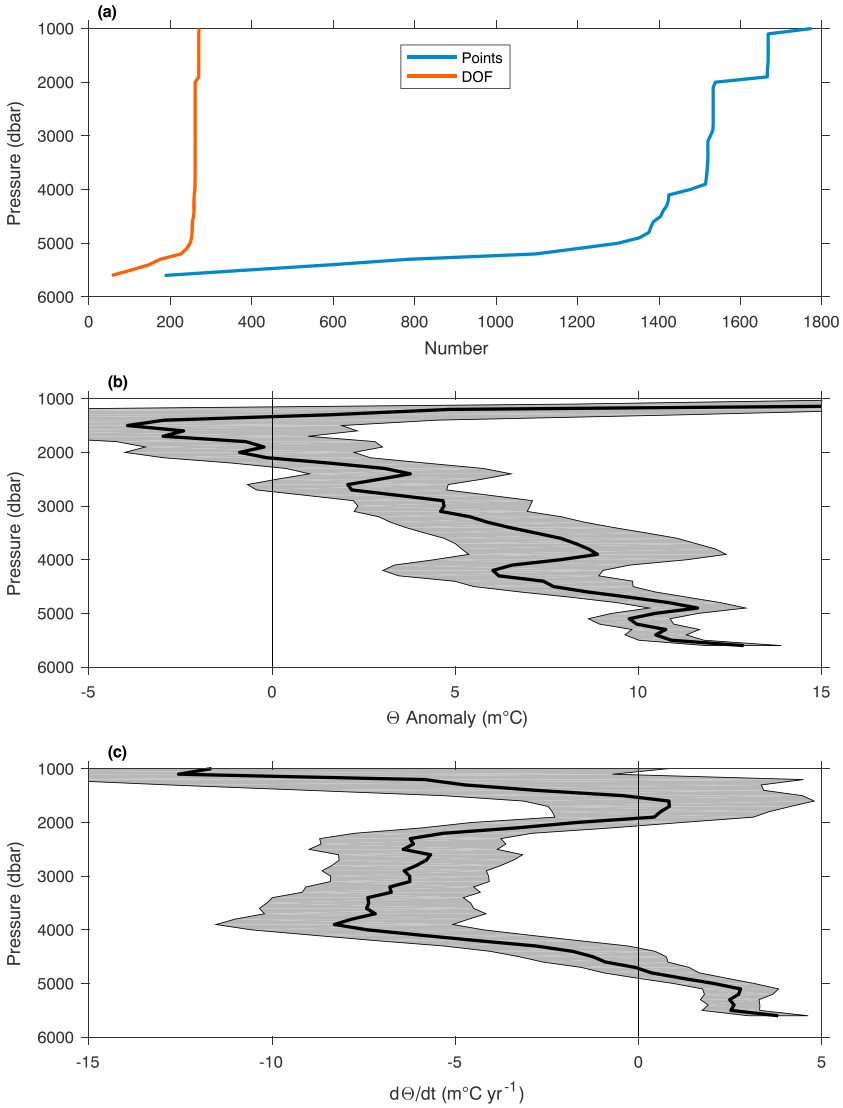

Figure 3. (a) Number of data points (blue line) and effective degrees of freedom (DOF) for linear fits versus time (red line) as a function of pressure in the Southwest Pacific Basin. (b) Anomaly (m°C) from linear fits (e.g., Figure 4) evaluated on 7 March 2017 relative to the World Ocean Atlas 2018 climatological average (thick black line) with 5–95% confidence limits (gray shading). (c) Trend of Θ (m°C/year) from the linear fits of Θ anomalies with 5–95% confidence limits (gray shading).

instance, WOA18 currently extends only to 5,500 m. Thus, 5,600 dbar, which is slightly shallower than that depth, is the maximum pressure level that we can consider here.

Next we fit a linear function versus time to the data from all the floats regardless of location for the Θ anomaly at each pressure level (e.g., Figure 4 at 5,100 dbar). We estimate the confidence limits on that trend in the standard fashion for unweighted least squares regressions (e.g., Wunsch, 1996, equation (3.3.10)). To estimate the effective degrees of freedom for these confidence limits, we assume that each float is far enough from its neighbors to be statistically independent (in terms of the dominant source of noise, mesoscale eddies) but that the data collected from each float are serially correlated in time, reducing the degrees of freedom. We use the 60-day decorrelation time scale estimated by Johnson et al. (2015), assuming that the values they calculated at 1,800 dbar did not change with increasing depth, as expected for the mesoscale waves and eddies that dominate the estimate. For example, if consecutive data points at a given pressure level from a float are separated in time by 60 days or more, they each are considered independent, but data points separated by 15 days would each contribute only one quarter of a degree of freedom subsequent to the single

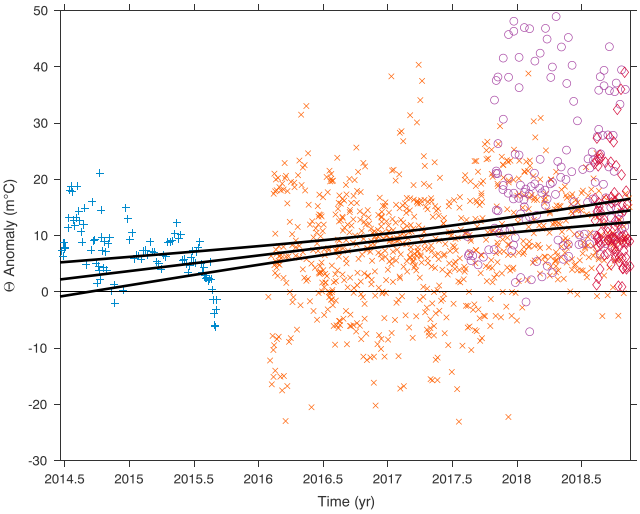

Figure 4. Anomalies of Θ for Deep Argo float data at 5,100 dbar in the Southwest Pacific Basin (Figure 1) from floats deployed in 2014 (blue plus symbols), 2016 (orange cross symbols), 2017 (purple circles), and 2018 (red diamonds) with respect the World Ocean Atlas 2018 long-term climatology with linear fit and 5–95% confidence limits (thick solid lines).

degree of freedom attributed to the initial data point in the time series. The floats used here have been cycling deep at 5, 10, or 15 days, typically, but more rapidly when making initial shallower profiles. Hence, applying these assumptions decreases the degrees of freedom by as little as a factor of ~3 around 5,600 dbar and as much as a factor of ~6 near 1,000 dbar, relative to the degrees of freedom assuming that each data point is statistically independent (Figure 3a).

We estimate the basin mean Θ anomalies at each pressure (Figure 3b) from the value of the linear fit versus time evaluated at the arithmetic mean of the profile dates (7 March 2017). We also estimate the basin-mean trend for Θ anomalies at each pressure (Figure 3c).

3. Results

Within the Southwest Pacific Basin there is a layer of very cold, nearly homogeneous, dense, water near the bottom (Figure 2) that is largely derived from Antarctic Bottom Water (Johnson, 2008). This layer can be several hundred meters thick over the abyssal plain, extending up to nearly 5,000 dbar. This water is also relatively fresh, oxygen-rich, and nutrient-rich compared to the saltier, nutrient-poorer water just above it (see Talley, 2007; World Ocean Circulation Experiment Section P15), indicating an increasingly higher fraction of North Atlantic Deep Water in the waters from the bottom to about 3,500 dbar (Johnson, 2008). From about 4,300 to 3,500 dbar, where salinity increases from deep to shallow (Talley, 2007), the vertical temperature gradient is stronger than either below 4,300 dbar or from 3,500 to 2,400 dbar (Figure 2c). From 3,500 to 2,400 dbar the vertical temperature gradient is again weaker (Figure 2c) and salinity decreases, oxygen decreases, and nutrient concentrations again increase with decreasing pressure indicating an increasing concentration of deep waters that have not been in contact with the atmosphere for centuries to millennia (e.g., Gebbie & Huybers, 2012; Khatiwala et al., 2012). Shallower than 2,400 dbar, the vertical temperature gradient (Figure 2c) again increases, indicating the gradual transition from deep waters toward intermediate and mode waters that are ventilated in the high latitudes and in much more recent contact with the atmosphere.

The difference from the long-term climatology is not statistically significantly different from zero from 1,200 to 2,200 dbar (Figure 3b). This absence of change is consistent with the centennial to millennial residence times of these waters. However, shallower than 1,200 dbar, the difference increases rapidly toward the surface, where it reaches several tenths of a degree Celsius (not shown) and more slowly toward the bottom where it last becomes statistically significantly different from zero at 95% confidence for pressures exceeding 2,800 dbar and reaches 11 (±1) m°C (Figure 3b) at a pressure of 5,500 dbar. These results are consistent with previous studies indicating both near-surface warming (e.g., Rhein et al., 2013) and increasingly statistically significant warming with increasing depth in the deep and bottom waters of the global ocean (e.g., Kouketsu et al., 2011; Purkey & Johnson, 2010).

The linear trend over the Deep Argo sampling period (4.4 years, from June 2014 to November 2018) is positive and statistically different from zero below 4,900 dbar, with average values of 3 (±1) m°C/year at pressures from 5,000 to 5,600 dbar (Figure 3c). The vertical temperature gradients are near zero at the lower portion of this pressure range (Figure 2). From 2,100 to 4,300 dbar, the trend also is statistically significant but negative, reaching a peak value of −8 (±3) m°C/year at 3,900 dbar (Figure 3c). The vertical temperature gradients in the layer that is cooling are larger than in the near-bottom layer that is warming (Figure 2). The gradients are largest near 3,900 dbar, where the peak negative value is located (Figure 3c).

4. Summary and Discussion

The abyssal layer of the Southwest Pacific Basin is at least 10 (±1) m°C warmer than the WOA18 long-term average (Figure 3b) in 2014–2018, as measured by 31 Deep Argo floats that are well dispersed throughout the region (Figure 1). Since the long-term average is a mean of maps for several decades, some of which might rely on sparse data, the time that this long-term average represents is difficult to determine, so the rate of

warming implied by this result is not clear. However, warming has been observed in the bottom waters of the basin at a rate around 1 m°C/year from the 1990s to the 2000s and 2 m°C/year from the 2000s to the 2010s (Purkey et al., 2019). From 2014 to 2018 the trend observed from 5,000 to 5,600 dbar is about 3 (±1) m°C/year, consistent with an acceleration in the rate of warming over time. The warming over the 4.4-year period is observed only in the coldest, densest, nearly vertically homogeneous waters, where no amount of vertical motion of isotherms could account for it. At 5,000 m, lateral motions of between roughly 40 and 200 km/year (roughly 1 to 6 mm/s), estimated using the range of local lateral gradients in the basin (Figure 1), are consistent with the changes. Hence, a very slight slowdown in the northward spread of Antarctic Bottom Waters could explain the contraction. A long-term reduction of the northward transport of bottom waters in the South Pacific has been inferred in at least two independent analyses of different data sets (Kouketsu et al., 2011; Voet et al., 2016).

Similarly, while the Deep Argo data show a bottom-intensified warm anomaly relative to the WOA18 climatology that is statistically different from zero starting at 2,300 dbar (Figure 3b), from 2014 to 2018, they measure a statistically significant cooling trend from 2100 to 4300 dbar, with a maximum rate of −8 (±3) m°C/year at 3,900 dbar (Figure 3c). This cooling is the equivalent of a vertical motion (in this case ascent), or heave, of deep isotherms of order 10 m/year. That heave could indicate a buildup of near-bottom water and deep water in the region; it could signal a change in the density structure associated with the geostrophic flow, or it could imply both.

We investigated the robustness of these results by subsetting the floats into six deployment periods (see symbol colors in Figures 1 and 4): 2014–2018 (all 31 floats, presented here), 2016–2018 (29 floats), 2014–2017 (21 floats), 2016–2017 (19 floats), 2014–2016 (13 floats), and even 2016 only (11 floats). The 2016 only subset has the advantage of multiple time series of similar record length all in the center of the analysis region, where lateral gradients are smaller in the bottom water. All of those analyses estimated similar statistically significant bottom-intensified warm anomalies, near-bottom warming trends, and deep cooling trends that largely overlap those presented here within 5–95% uncertainties. These results increase confidence in the findings presented here.

While the temperature sensors are thought to be accurate to order 1 m°C, results presented here are robust even if random normally distributed temperature offsets with a standard deviation of 5 m°C (substantially larger than expected calibration errors) are applied to data from each float. As already mentioned, for data from the few floats with substantial errors in salinity measurements, replacing bad salinity values with those estimated using a polynomial deep temperature-salinity relation could introduce a maximum error of 1 m°C in computed Θ values, similar to the measurement error for temperature. However, the community has less experience with the pressure sensors used on Deep Argo floats, and the early floats may have pressure calibration errors. The effect of a 1-dbar error (with the float reporting a higher pressure that truth) on calculation of conservative temperature owing to the compressibility of seawater is roughly −0.1 m°C/dbar. In the homogenous near-bottom layer, that would be the main source of error since the vertical gradient of conservative temperature is negligible. However, in the more stratified region the effect of a pressure sensor error owing to the vertical temperature gradient would oppose the thermodynamic effect and could be as large as 0.6 m°C/dbar of pressure error. Since float calibration errors could be on the order of several decibars at high pressures and cold temperatures, the results in the more stratified deep waters should be regarded with some caution.

One additional possible source of uncertainty that is not considered here is the use of a mixed-era climatology. While the WOA18 mean climatology is carefully constructed from decadal averages, in the deep and bottom waters the sampling is sparse even when combining all data for any one decade, so spatial and temporal variability are likely aliased in the climatology. Locally, this might make trends in anomalies suspect as the floats are deployed in different locations at different times or if they move from one location to the other. For instance, the warm anomalies at 5,100 dbar for floats deployed in 2017 mostly along the eastern edge of the array (purple o's in Figures 1 and 4) could be real or a manifestation of such an artifact. However, the ensemble of 31 float trajectories is somewhat random (Figure 1), so that aliasing is likely to be largely averaged out over the basin scale, which is one reason the analysis is done on that large scale. After a global Deep Argo array is established, it will allow estimation of a much superior climatology from a single era, as well as assessment of the seasonal cycle in the deep ocean (which is likely to be small in deep midlatitudes away

from the western boundary). Longer records from individual Deep Argo floats will also allow independent estimates of the decorrelation time scales at these depths, testing the hypothesis that they result from mesoscale eddies and waves and hence are largely independent of depth. With these improvements estimations of local anomalies and trends relative to the deep Argo climatology will be more reliable.

The time period over which these trends are calculated, 4.4 years, is rather short to infer much about long-term changes. Nonetheless, this analysis does demonstrate that an array of Deep Argo floats maintained at near the 5° latitude × 5° longitude (Figure 1) recommended density (Johnson et al., 2015) is able to resolve regional (basin-scale) deep temperature changes with high statistical confidence over a relatively short (less than pentadal) time period. That ability is unprecedented on a regional scale in the deep and bottom waters. In addition, the 4.4-year warming trend in the bottom waters suggests an accelerated bottom water warming relative to that observed in the region between the 1990s and the 2010s (Purkey et al., 2019). The Deep Argo array, when global, will provide even more insights into the mean state and changing properties of deep and bottom waters and variations in their circulation.

Acknowledgments
G. C. J. is supported by the Global Ocean Monitoring and Observing program, National Oceanic and Atmospheric Administration (NOAA), and U.S. Department of Commerce and NOAA Research. Participation by N. Z. was supported by SIO CIMEC Argo (NOAA grant NA15OAR4320071) and NOAA (NA18OAR0110434). We are grateful for the hard work of the engineers and scientists who developed the Deep Argo floats; the scientists, officers, and crew of all the cruises on which they were deployed; and those who pilot the floats, make their data publically available, and quality control them. Two anonymous reviewers provided constructive suggestions that improved the manuscript. PMEL contribution 4897. The WOA climatology was downloaded from https://www.nodc.noaa.gov/OC5/woa18/, and the Deep Argo data were downloaded from https://www.usgodae.org/argo/argo.html on 20 November 2018.

References

Aoki, S., Kitade, Y., Shimada, K., Ohshima, K. I., Tamura, T., Bajish, C. C., et al. (2013). Widespread freshening in the seasonal ice zone near 140°E off the Adélie land coast, Antarctica, from 1994 to 2012. *Journal of Geophysical Research: Oceans*, *118*, 6046–6063. https://doi.org/10.1002/2013JC009009

Boé, J., Hall, A., & Qu, X. (2009). Deep ocean heat uptake as a major source of spread in transient climate change simulations. *Geophysical Research Letters*, *36*, L22701. https://doi.org/10.1029/2009GL040845

Desbruyères, D. G., Purkey, S. G., McDonagh, E. L., Johnson, G. C., & King, B. A. (2016). Deep and abyssal ocean warming from 35 years of repeat hydrography. *Geophysical Research Letters*, *43*, 10,356–10,365. https://doi.org/10.1002/2016GL070413

Gebbie, G., & Huybers, P. (2012). The mean age of ocean waters inferred from radiocarbon observations: Sensitivity to surface sources and accounting for mixing histories. *Journal of Physical Oceanography*, *42*(2), 291–305. https://doi.org/10.1175/JPO-D-11-043.1

Hartmann, D. L., Klein Tank, A. M. G., Rusticucci, M., Alexander, L. V., Brönnimann, S., Charabi, Y., et al. (2013). Observations: Atmosphere and surface. In T. F. Stocker et al. (Eds.), *Climate change 2013: The physical science basis. Contribution of working group I to the fifth assessment report of the Intergovernmental Panel on Climate Change* (pp. 159–254). Cambridge, United Kingdom and New York: Cambridge University Press. https://doi.org/10.1017/CBO9781107415324.008

IOC, SCOR and IAPSO (2010). The international thermodynamic equation of seawater - 2010: Calculation and use of thermodynamic properties. Intergovernmental Oceanographic Commission, manuals and guides no. 56, UNESCO (English), 196 pp.

Jayne, S. R., Roemmich, D., Zilberman, N., Riser, S. C., Johnson, K. S., Johnson, G. C., & Piotrowicz, S. R. (2017). The Argo program: Present and future. *Oceanography*, *30*(2), 18–28. https://doi.org/10.5670/oceanog.2017.213

Johnson, G. C. (2008). Quantifying Antarctic Bottom Water and North Atlantic Deep Water volumes. *Journal of Geophysical Research*, *113*, C05027. https://doi.org/10.1029/2007JC004477

Johnson, G. C., Lyman, J. M., Boyer, T., Cheng, L., Domingues, C. M., Gilson, J., et al. (2018). Global oceans: Ocean heat content. In state of the climate in 2017. *Bulletin of the American Meteorological Society*, *99*(8), Si–S310. https://doi.org/10.1175/2018BAMSStateoftheClimate.1

Johnson, G. C., Lyman, J. M., & Loeb, N. G. (2016). Improving estimates of Earth's energy imbalance. *Nature Climate Change*, *6*(7), 639–640 . https://doi.org/10.1038/nclimate3043

Johnson, G. C., Lyman, J. M., & Purkey, S. G. (2015). Informing Deep Argo array design using Argo and full-depth hydrographic section data. *Journal of Atmospheric and Oceanic Technology*, *32*(11), 2187–2198. https://doi.org/10.1175/JTECH-D-15-0139.1

Khatiwala, S., Primeau, F., & Holzer, M. (2012). Ventilation of the deep ocean constrained with tracer observations and implications for radiocarbon estimates of ideal mean age. *Earth and Planetary Science Letters*, *325-326*, 116–125. https://doi.org/10.1016/j.epsl.2012.01.038

Kobayashi, T. (2018). Rapid volume reduction in Antarctic Bottom Water off the Adélie/George V Land coast observed by deep floats. *Deep-Sea Research Part I: Oceanographic Research Papers*, *140*, 95–117. https://doi.org/10.1016/j.dsr.2018.07.014

Kouketsu, S., Doi, T., Kawano, T., Masuda, S., Sugiura, N., Sasaki, Y., et al. (2011). Deep ocean heat content changes estimated from observation and reanalysis product and their influence on sea level change. *Journal of Geophysical Research*, *116*, C03012. https://doi.org/10.1029/2010JC006464

Newsom, E. R., Bitz, C. M., Bryan, F. O., Abernathey, R., & Gent, P. R. (2016). Southern ocean deep circulation and heat uptake in a high-resolution climate model. *Journal of Climate*, *29*(7), 2597–2619. https://doi.org/10.1175/JCLI-D-15-0513.1

Oka, E., & Ando, K. (2004). Stability of temperature and conductivity sensors of Argo profiling floats. *Journal of Oceanography*, *60*(2), 253–258. https://doi.org/10.1023/B:JOCE.0000038331.10108.79

Orsi, A. H., Johnson, G. C., & Bullister, J. L. (1999). Circulation, mixing, and production of Antarctic Bottom Water. *Progress in Oceanography*, *43*(1), 55–109. https://doi.org/10.1016/S0079-6611(99)00004-X

Purkey, S. G., & Johnson, G. C. (2010). Warming of global abyssal and deep Southern Ocean waters between the 1990s and 2000s: Contributions to global heat and sea level rise budgets. *Journal of Climate*, *23*(23), 6336–6351. https://doi.org/10.1175/2010JCLI3682.1

Purkey, S. G., & Johnson, G. C. (2013). Antarctic Bottom Water warming and freshening: Contributions to sea level rise, ocean freshwater budgets, and global heat gain. *Journal of Climate*, *26*(16), 6105–6122. https://doi.org/10.1175/JCLI-D-12-00834.1

Purkey, S. G., Johnson, G. C., & Chambers, D. P. (2014). Relative contributions of ocean mass and deep steric changes to sea level rise between 1993 and 2013. *Journal of Geophysical Research: Oceans*, *119*, 7509–7522. https://doi.org/10.1002/2014JC010180

Purkey, S. G., Johnson, G. C., Talley, L. D., Sloyan, B. M., Wijffels, S. E., Smethie, W., et al. (2019). Unabated Bottom Water Warming and Freshening in the South Pacific Ocean. *Journal of Geophysical Research: Oceans*, *124*. https://doi.org/10.1029/2018JC014775

Rhein, M., Rintoul, S. R., Aoki, S., Campos, E., Chambers, D., Feely, R. A., et al. (2013). Observations: Ocean. In T. F. Stocker et al. (Eds.), *Climate change 2013: The physical science basis. Contribution of working group I to the fifth assessment report of the Intergovernmental*

Panel on Climate Change (pp. 255–316). Cambridge, United Kingdom and New York: Cambridge University Press. https://doi.org/10.1017/CBO9781107415324.010

Rintoul, S. R. (2007). Rapid freshening of Antarctic Bottom Water formed in the Indian and Pacific oceans. *Geophysical Research Letters*, *34*, L06606. https://doi.org/10.1029/2006GL028550

Roemmich, D., Church, J., Gilson, J., Monselesan, D., Sutton, P., & Wijffels, S. (2015). Unabated planetary warming and its ocean structure since 2006. *Nature Climate Change*, *5*(3), 240–245. https://doi.org/10.1038/nclimate2513

Smith, W. H. F., & Sandwell, D. R. (1997). Global seafloor topography from satellite altimetry and ship depth sounding. *Science*, *277*(5334), 1956–1962. https://doi.org/10.1126/science.277.5334.1956

Talley, L. D. (2007). In M. Sparrow, P. Chapman, & J. Gould (Eds.), *Hydrographic atlas of the world ocean circulation experiment (WOCE). Volume 2: Pacific Ocean*. Southampton, UK: International WOCE Project Office.

Talley, L. D., Feely, R. A., Sloyan, B. M., Wanninkhof, R., Baringer, M. O., Bullister, J. L., et al. (2016). Changes in ocean heat, carbon content, and ventilation: A review of the first decade of GO-SHIP global repeat hydrography. *Annual Review of Marine Science*, *8*(1), 185–215. https://doi.org/10.1146/annurev-marine-052915-100829

Voet, G., Alford, M. H., Girton, J. B., Carter, G. S., Mickett, J. B., & Klymak, J. M. (2016). Warming and weakening of the abyssal flow through Samoan passage. *Journal of Physical Oceanography*, *46*(8), 2389–2401. https://doi.org/10.1175/JPO-D-16-0063.1

Wunsch, C. (1996). *The Ocean Circulation Inverse Problem*. Cambridge, UK: Cambridge University Press. https://doi.org/10.1017/CBO9780511629570